

Use of Landsat 8 OLI and Aeromagnetic Data for Structural Mapping of Pako Basin Region, North Benin

Raoufou D. Ibrahim GNAMMI YORO^{1,*}, Gérard Alfred Franck d'ALMEIDA¹,
Karim ALLEK², Christophe KAKI¹, Nicaise YALO³

¹Laboratory of Geology, Mines and Environment, Department of Earth Sciences, University of Abomey-Calavi,
01 BP 4521 COTONOU (R. Benin)

²Geophysics Laboratory, Department of Geophysics, M'Hamed Bougara-Boumerdes University,
Avenue de l'Indépendance 35000 Boumerdes, Algeria

³National Institute of Water (INE / UAC), 01 BP 526 Cotonou (R. Benin)

*Corresponding author: ygnammi85@yahoo.com

Received May 14, 2020; Revised June 16, 2020; Accepted June 22, 2020

Abstract Spectral geology and aeromagnetic data help geoscientists in mapping and prediction of potential mineral areas. This paper aims to present structural features of the poorly studied Pako region of northern Benin using Landsat 8 OLI images and aeromagnetic data. Remote sensing technique led to the discovery of several faults of two main directions (N-S and E-W), resulting from great regional tectonics' deformations. The other faults have NE-SW to NW-SE orientations. Among identified faults, N-S faults (N18°) gathering 14% and E-W (N92°) to NW-SE (N160°) fractures cumulating 61% limit the basin on both sides. Therefore, these faults could be interpreted as border fractures which have initiated the formation of Pako basin. Total magnetic field technique held to define anomalous zones and associate shears zones in order to identify potential corridors of mineralization. Field observations in Pako region have confirmed the existence of brittle deformations, as sociated to dextral and/or senestral detachment, and ductile deformations with rotational dextral components. The integration of our results with the regional geological context allow to propose a structural model of Pako region.

Keywords: Landsat 8 OLI, aeromagnetic data, Pako region, faults, structural model.

Cite This Article: Raoufou D. Ibrahim GNAMMI YORO, Gérard Alfred Franck d'ALMEIDA, Karim ALLEK, Christophe KAKI, and Nicaise YALO, "Use of Landsat 8 OLI and Aeromagnetic Data for Structural Mapping of Pako Basin Region, North Benin." *Journal of Geosciences and Geomatics*, vol. 8, no. 2 (2020): 45-57 doi: 10.12691/jgg-8-2-1.

1. Introduction

Remote sensing technology plays an important role in geological mapping and provides opportunity to investigate the remote areas of the earth's surface. Magnetic survey is an important geophysical technique that is particularly suitable for surface and subsurface investigations. Thus, satellite images and magnetic data allow to discriminate linear structures and rock units. They are also useful to establish reasonable correlations between structures and rocks units identified on earth surface and their continuities in depth [1-7]. Landsat images and geophysical data have shown that western and eastern blocks of Dahomeyids Panafrikan chain are connected by important geological structures [8,9]. These structures form large, decaying shear zones of general direction N-S to NE-SW related to the genesis and deformation of Neoproterozoic granites [9]. In the Western Bloc of Nigeria, these shear zones are closely associated with spatial distribution and deformation of schists chains which include corridors

carrying interesting mineralization. For example, Anka shear corridor (Nigeria) represents an important gold mineralization that extends to Maradi region (Niger Republic) [10,11,12]. Until that day, geological prospecting in the northern part of Benin didn't yet highlight some corridors of mineralization, however this part of the country, which include the Pako region, has a similar geological history with western Nigeria. The Pako volcano-sedimentary basin has been subject of some limited prospecting work because the National fauna Park W covers a large part of this basin [13,14]. Based on Landsat 8 image, aeromagnetic data and field observations, the present study aims to provide more informations for better structural characterization of Pako region.

2. Geological Setting

Located in Alibori department (North Benin) and delimited by latitudes North 11° and 12° and longitudes East 2° and 3°, the Pako region, partially covers Banikoara and Karimama municipalities (Figure 1).

The study area is devoid of significant relief and characterized by a migmatitic gneissic basement, containing schists, metasediments, volcanites and intruded granites (Figure 2).

Rocks of the region can be grouped in three major lithotectonic units [8,9,16-20]:

- a migmatitic gneiss complex unit of Archean age marked by several metamorphic events between 3.1 and 0.6 Ga and intruded by Panafrican calco alkaline granites;
- a schists chains unit composed of metasediments, green schists and amphibolite facies;
- a Neoproterozoic granites unit [8,9].

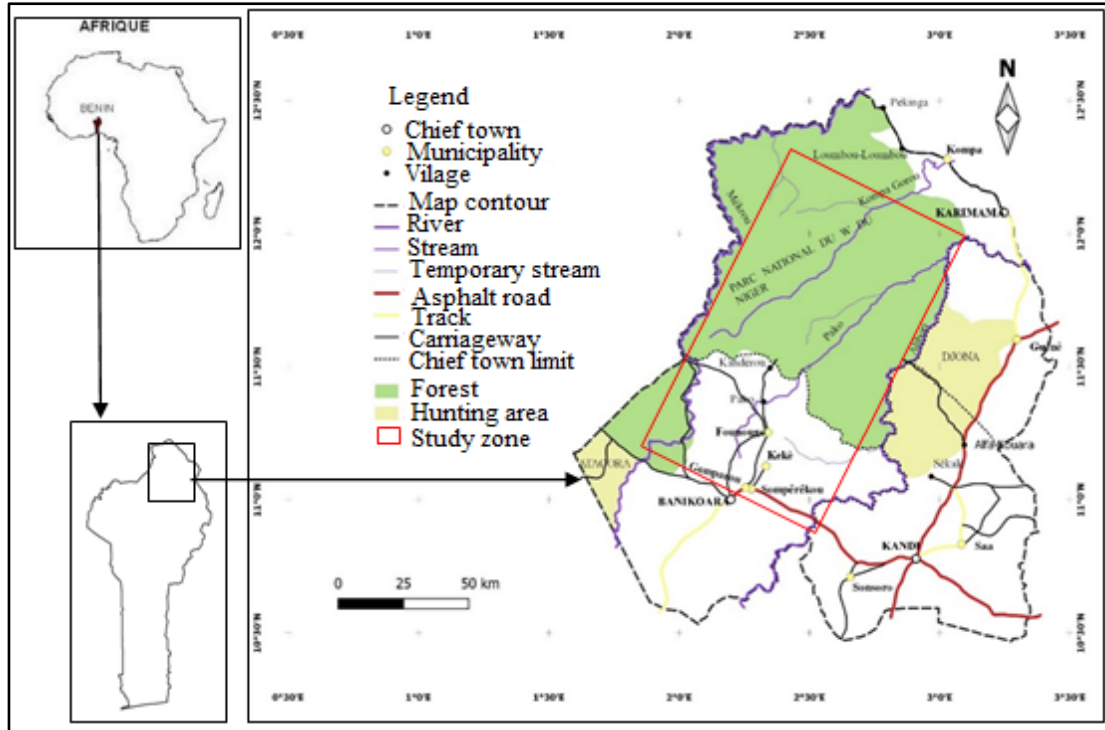


Figure 1. Location of the study area [15]

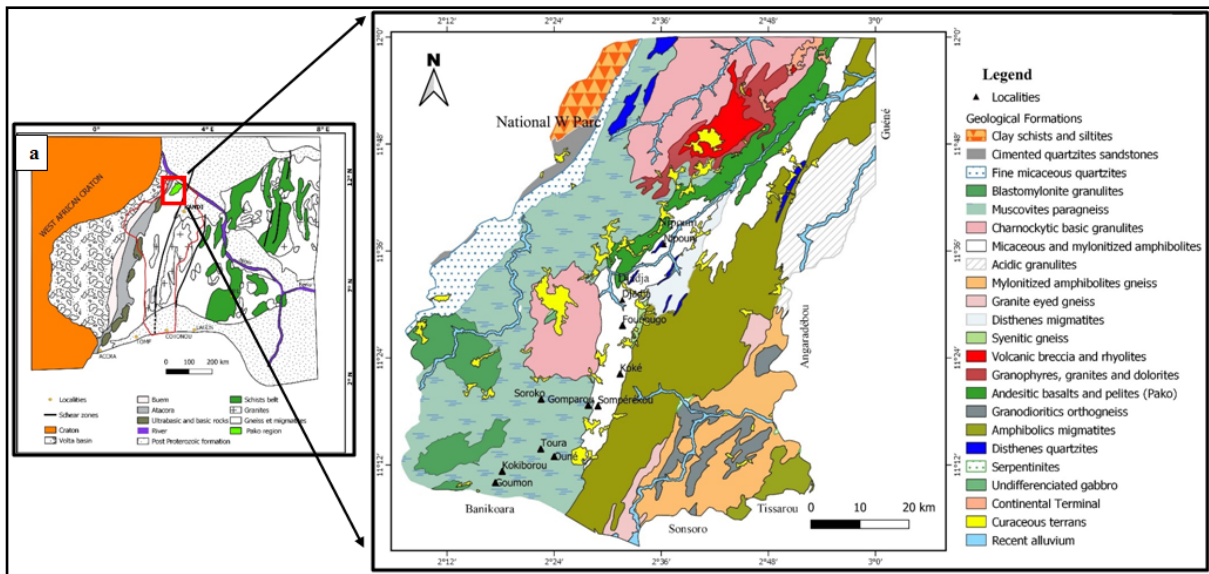


Figure 2. Geological map of Pako basin region a) Regional context b) local context [14,22]

3. Material and Methods

3.1. Types of Used Data

- Landsat 8 OLI (Operational Land Imagery) image (LC08_L1TP_192052) free downloaded from <http://earthexplorer.usgs.gov/>;
- Aeromagnetic data in raster format available at Beninese Office of Geological and Mining Research.

These data were obtained after a geophysical campaign held in March 1966 by Prakla [13]. For data acquisition, spacing between flight lines was five hundred (500) meters with a maximum tolerance of seven hundred (700) meters;

- Geological maps at 1 / 200,000 of northern part [14] and tourist maps of Benin [15].

The characteristics of the spectral bands are presented in the Table 1.

Table 1. Characteristics of the spectral bands of Landsat 8 OLI

Captors	Spectrales Bands	Wave length	Resolution
OLI	Band 1 - Aérosols	0,433 - 0,453 μm	30 m
	Band 2 - Blue	0,450 - 0,515 μm	30 m
	Band 3 - Green	0,525 - 0,600 μm	30 m
	Band 4 - Red	0,630 - 0,680 μm	30 m
	Band 5 - Near infrared	0,845 - 0,885 μm	30 m
	Band 6 - Medium infrared 1	1,560 - 1,660 μm	30 m
	Band 7 - Medium infrared 12	2,100 - 2,300 μm	30 m
	Band 8 - Panchromatic	0,500 - 0,680 μm	15 m
	Band 9 - Cirrus	1,360 - 1,390 μm	30 m
TIRS	Band 10 - Infrared moyen 1	10,30 - 11,30 μm	100 m
	Band 11 - Infrared moyen 2	11,50 - 12,50 μm	100 m

Each type of data has been subject to specific processing.

3.2. Processing Methods

Landsat 8 OLI images were processed by Sobel 7x7 directional filters in order to improve artifacts and facilitate the manual extraction of lineaments in accordance with the process defined by [24,25,26]. After hydrographic network analysis, the interpretation method consisted in search of various alignments and small traces underlined by tonal contrasts of the light or dark streaks and abrupt change of slopes. An automatic extraction carried out on the first Principal Component (ACP1) of the first seven bands of Landsat 8 image, allows to draw up a density map of lineaments network [27,28,29,30]. The superposition of results of manual and automatic extraction of lineaments helped to detect a considerable number of joints, fractures or faults. Treatments were done using Envi 5.1, Geomatica 2015 and QGIS3.4 software platforms. Lineaments directions were discriminated by Georse software.

Aeromagnetic data processing started with total magnetic field data generation using GIS [13]. Taking into account the geographic position of the study area, method of total magnetic field reduction to equator was adopted [1]. Thus, to reduce the magnetic data to equator; equation (1) was applied:

$$L(\theta) = \frac{\left\{ \begin{array}{l} \left[\sin(I) - i \cos(I) \cdot \cos(D - \theta) \right]^2 \\ \times \left(-\cos^2(D - \theta) \right) \end{array} \right\}}{\left\{ \begin{array}{l} \left[\sin^2(Ia) + \cos^2(Ia) \cdot \cos^2(D - \theta) \right] \\ \times \left[\sin^2(I) + \cos^2(I) \cdot \cos^2(D - \theta) \right] \end{array} \right\}} \quad (1)$$

where:

$L(\theta)$ = TMI Reduction to Equator (RTE);

I = geomagnetic inclination;

Ia = inclination for amplitude correction (never < 1);

D = geomagnetic declination.

When reducing to equator from low latitudes, North-South features can blow-up due to the numerical error (from the term of 0/0) in amplitude correction (the

$\sin(I)$ component) that is applied when (D -) is $\delta/2$ (i.e. a magnetic east-west wave number). By specifying higher latitude for the amplitude correction alone, this problem can be reduced or eliminated at the expense of slightly under-correcting the amplitudes of near North-South features. The following parameters obtained from geomagnetic calculator (IGRF) were used for RTE:

Table 2. Parameters from IGRF (International Geomagnetic Reference Field) of the study area in 1966

D (°)	I (°)	F (nT)	H (nT)	X (nT)	Y (nT)	Z (nT)
-7	3.5	32463	32875	32644	-3890	2186

The horizontal (x, y) and vertical (z) gradients were applied to the reduced magnetic field data to equator [31]. These different processes allowed to get maximum amount of informations concerning magnetic structures, maps, structural discontinuities and confirm certain results obtained from spatial data.

The horizontal derivative enhances high frequency variation of magnetic data. These variations can be caused by faults and/or boundaries between different geological units. Horizontal derivative is useful for detecting or interpreting rocks features. In spatial domain, the horizontal gradient method of magnetic field $F(x, y)$ defined at different points (x, y) of the horizontal plane of measurement, is given by the relation of [31].

$$HG(x, y) = \sqrt{\left(\frac{\partial F}{\partial x} \right)^2 + \left(\frac{\partial F}{\partial y} \right)^2} \quad (2)$$

However, the vertical derivative is commonly applied to total magnetic field data to enhance the shallow geologic sources and suppress deeper ones. The computational relation of vertical derivative is giving by equation (3).

$$\phi(x_1 y, z_0) = f_{(x,y,z_0)}^{(n_1)} + w(x, y) f_{(x,y,z_0)}^{(n_2)}. \quad (3)$$

MAGMAP extension of Geosoft 6.4 software (Oasis Montaj) served as a platform for the various treatments.

This technique applies 2D Fast Fourier Transform (FFT) approach on magnetic data.

The relevance and consistency of ours results will be established after control and validation with field data. Thus, geological map of the study area is compared with linear structures extracted from satellite images and aeromagnetic data in order to infer their structural meaning [32]. The proven anthropogenic lineaments (roads, tracks, limits of forests or cultivated areas, power lines, etc.) are removed and the remaining lineaments are considered as fractures. The verification process is supported by field observations and structural measurements.

4. Results and Discussion

4.1. Results

4.1.1. Extraction of lineaments

Sobel filters have the particularity to enhance lineaments perpendicular to their convolution direction. Sobel filter of N-S (0°) direction accentuates linear structures of E-W (90°) and NE-SW directions. Sobel filter of NE-SW(45°) direction accentuates NW-SE and E-W steering accidents. Sobel filter of E-W (90°) direction highlights direction N-S and NW-SE. Manually

lineaments extraction results are presented in Figure 3. The synthesis of manual extraction process enabled to create linear map of Pakovolcano-sedimentary basin region (Figure 4). On this map, one hundred and seventy-one (171) lineaments of varied direction and length (683 m to 13.63 km) were represented.

Detailed analysis of this map shows that some sectors are apparently less fractured and extracted lineaments are globally of five directions. lineaments, which follow each other in the same direction suggest a same zone of weakness (Figure 4). They are structural lineations (schistosity and/or foliation planes; shear or foldszones).

Rosace of lineaments directions automatically generated by Georse software showed five main directions: $N40^\circ$, $N55^\circ$, $N72^\circ$, $N120^\circ$ and $N160^\circ$ (Figure 5a). These lineaments directions can be grouped into: i) NE-SW ($N40^\circ$ to $N55^\circ$); ii) the E-W ($N72^\circ$) and iii) NW-SE ($N120^\circ$ to $N160^\circ$). N-S direction ($N0^\circ$ to $N20^\circ$) is poorly represented.

Statistical analysis of lineaments groups indicates that NE-SW orientation is predominant, with 45.03% of the lineaments; NW-SE direction gather 28.65%; E-W direction represents 13.45% and N-S direction accounts for 12.87% (Figure 5b). Remote sensing results allow us to conclude that NE-SW lineaments have played an important role in the actual configuration of Pako region.

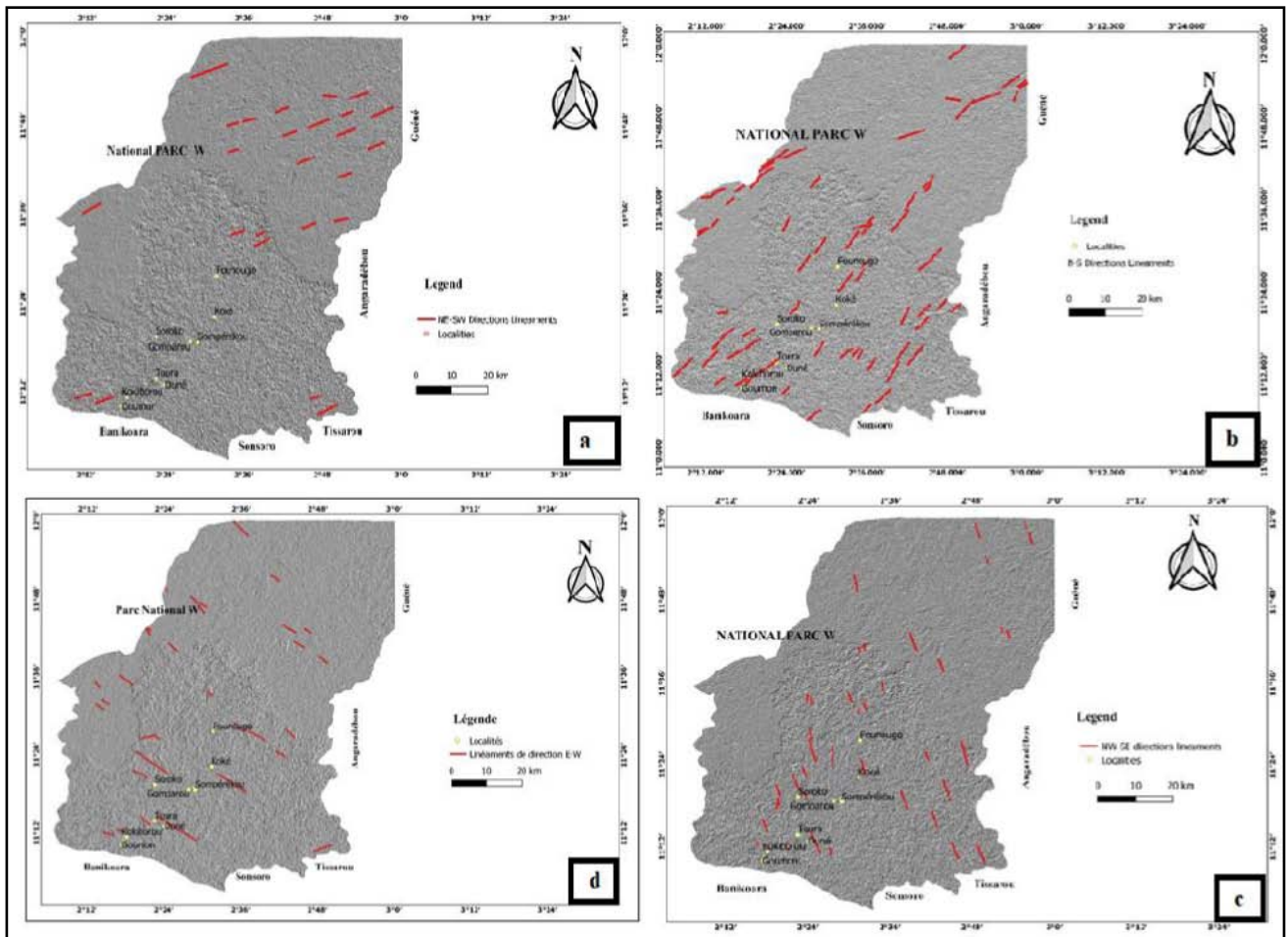


Figure 3. Sobel directional filters maps a) NW-SE b) E-W c) NE-SW d) N-S

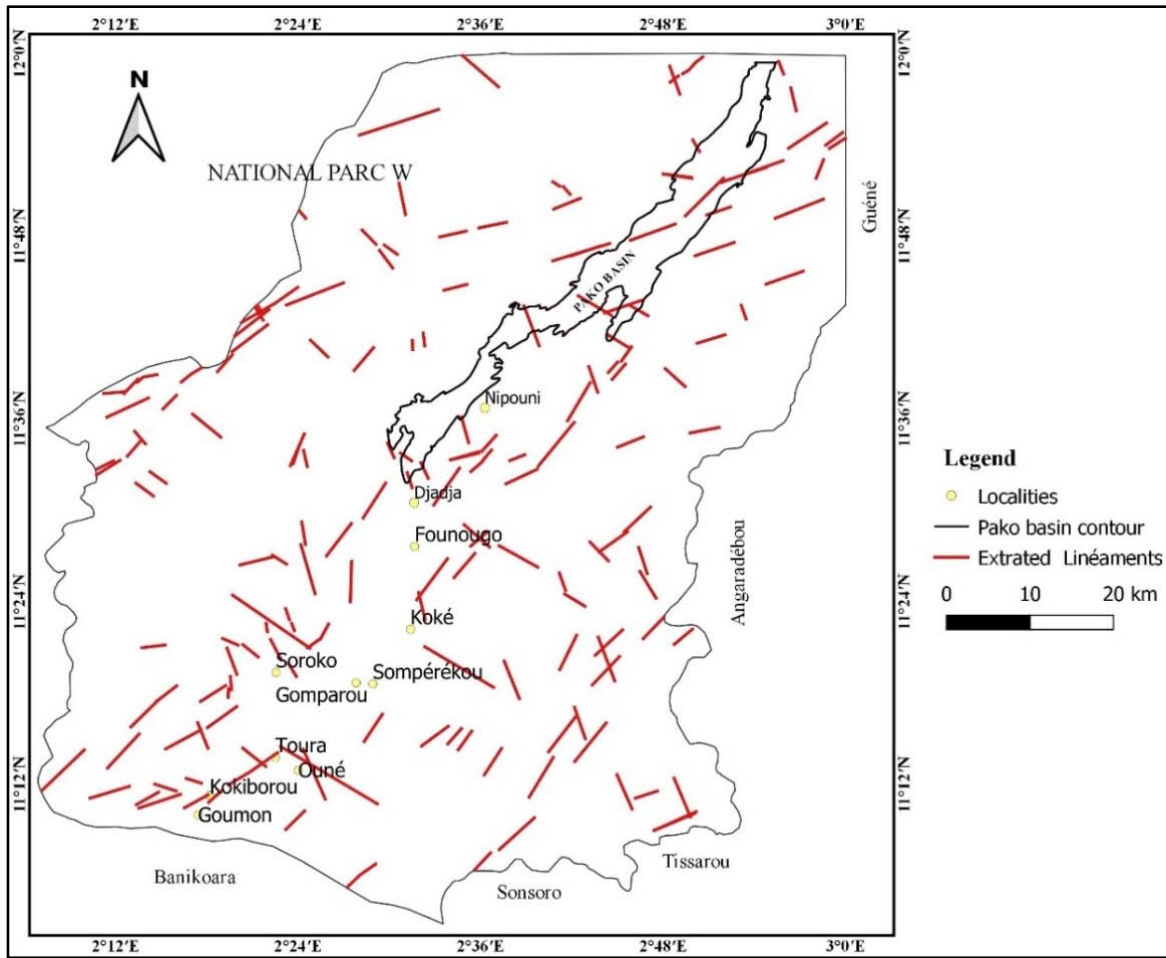


Figure 4. Extracted lineaments map of Pako region

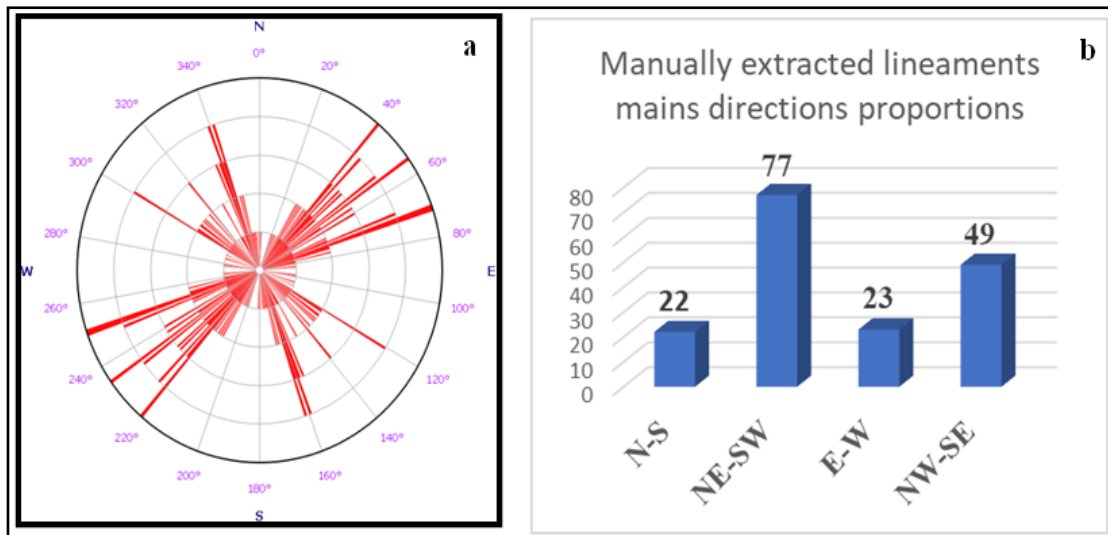


Figure 5. Pako region lineaments main directions: a) Rosace diagram; b) histogram of directions

4.1.2. Intensity of Fracturing Network in Pako Region

The fractures are distributed differently in Pako region. The areas of high linear density are found in the southern sector of Pako basin and neighboring regions up to Nipouni (Figure 6). The northern sector seems to be less fractured due to the presence of athick vegetation of National fauna Park W. The overlay of manually extracted lineaments map with the density map of the automatically generated fracturing network shows that highly fractured

zones are concentrated on the red color zones of the density map while, meanly fractured areas are concentrated in yellow zone. Weakly fractured areas and areas without fracturation are concentrated in green and white color zone respectively (Figure 6). Areas, where satellite could not collect enough data to provide structural information correspond to sectors covered by National fauna Park W, hunting areas of Djona and Atacora (see Figure 1).

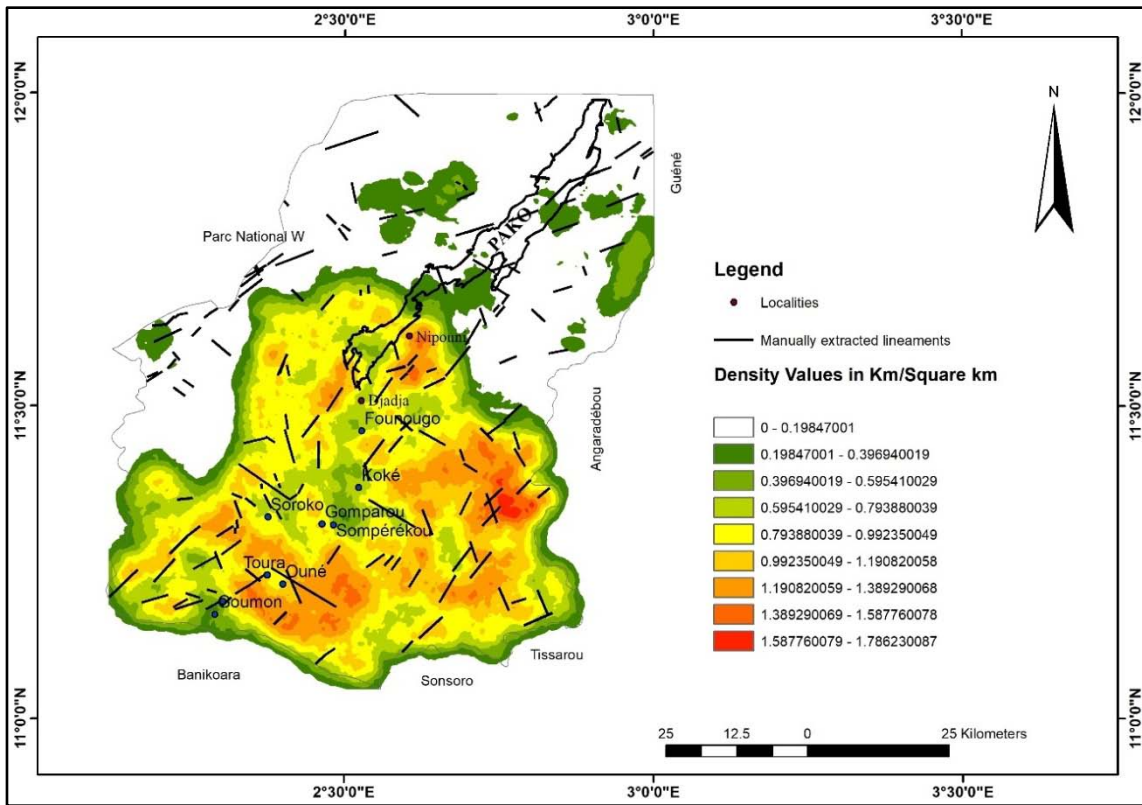


Figure 6. Fracture density map of Pako region

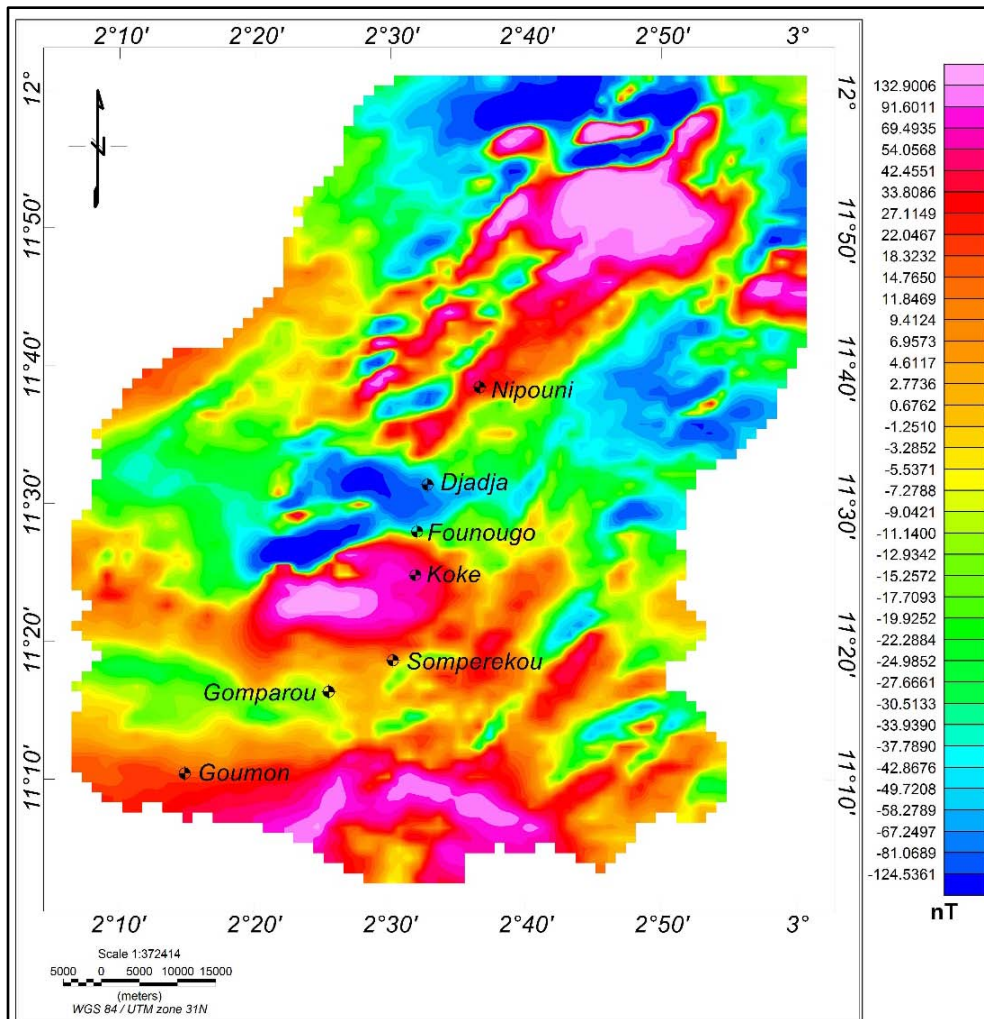


Figure 7. Map of reduction to equator of the CMT of Pako region

4.1.3. Reduction to Equator (RTE) of Total Magnetic Field (TMF)

Reducing the TMF (Total Magnetic Field) to equator has contributed to make anomalies symmetrical with respect to their sources and to re-specify their contours. Analysis of the map shows a range of intensity variation between -124.54 nT and 132.90 nT. The zones between 54.05 nT and 132.90 nT are zones with very high magnetic intensity, those between 0.7 nT and 42.45 nT of medium magnetic intensity and zones with values between -1.25 nT and -49.72 nT, are weedy intensity magnetic. Anomalous values between -58.28 nT and -124.54 nT, are very low magnetic intensity. However, in low latitudes magnetic regions, specifically around the equator, a low or negative magnetic peak value represents typical abnormal signatures. Consequently, we can recognize in Pako region four (4) major geological processes in relation to the recognized anomalous zones.

The central sector of Pako is characterized by a very high magnetic anomaly and the Nipouni sector shows

anomalies of medium, low to very low magnetic intensity. There are very low values of magnetic intensity in the Djadja sector structured E-W and NE-SW (Figure 7). In South of Pako region, the magnetic anomalies are high moderate but very discontinuous.

4.1.4. Horizontal Gradient (X-derivative)

The component (x) of horizontal gradient of magnetic anomaly reduced to equator allows highlighting N-S linear structures of short lengths. It enhances faults and geological contacts (lithological and tectonic). Analysis of (x) derivative map shows that in Pako region, the axes of both negative and positive anomalies are globally oriented NE-SW (Figure 8). Two major directions (E-W and NW-SE) characterize fractures identified on this map. They are totally discordant with N-S to NE-SW faults directions which are linked to Panafrican orogeny. NW-SE to E-W could be related to tectonic evolution of Pako volcano-sedimentary basin. They represent the southern border faults of Pako basin in Djadja region (Figure 8).

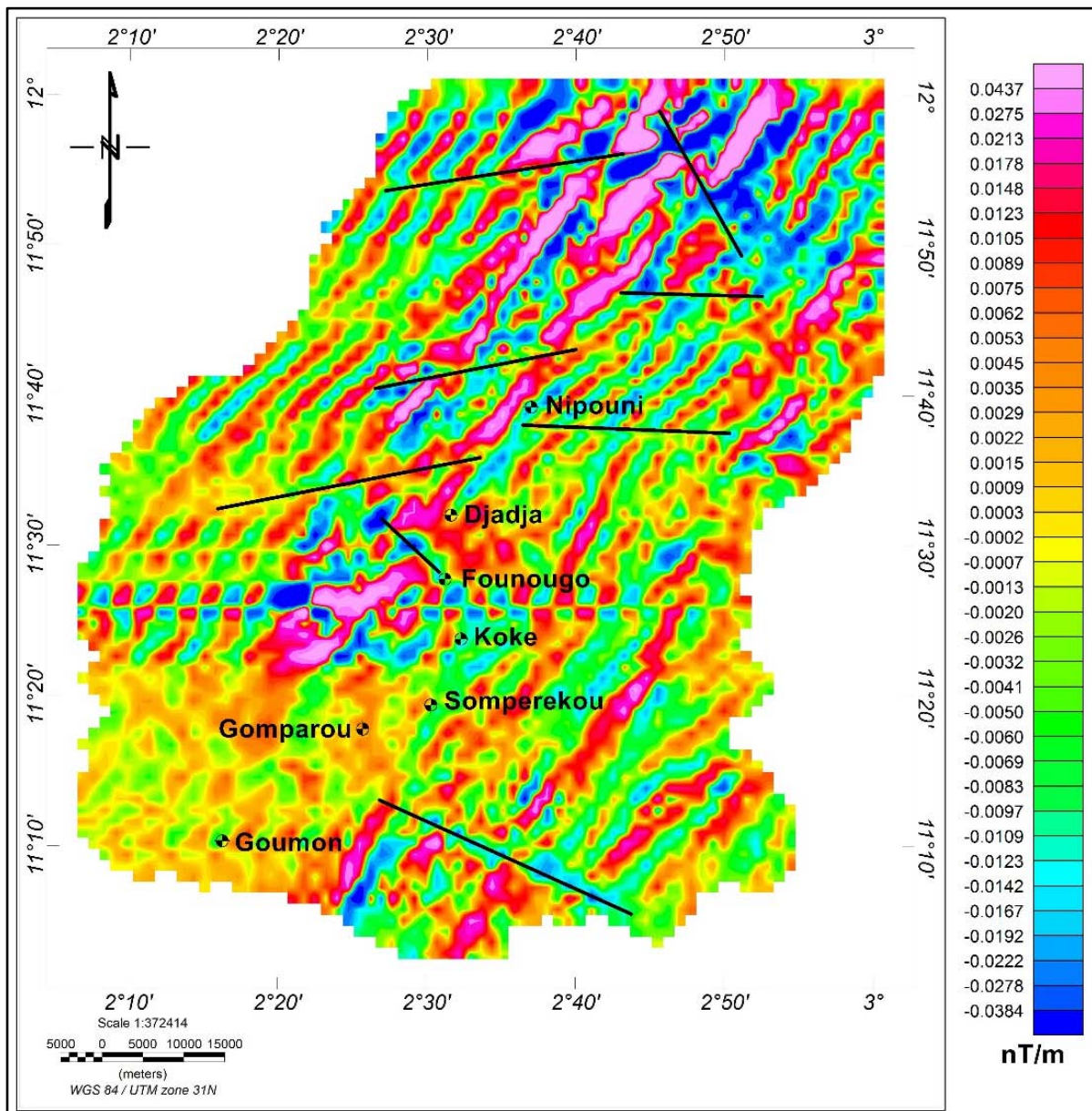


Figure 8. Map of horizontal (x) derivative of total magnetic field reduced to equator in Pako region

4.1.5. Horizontal Gradient (Y-Derivative)

The component (y) of horizontal gradient consists in suppressing anomalies of long wavelengths to highlight oriented E-W structures of short wavelengths. Within the framework of the present study, it highlights structures with very weedy negative anomalies in further north and Founougo sectors (Figure 9). NE-SW direction of structures are observed in the whole Pakoregion. Several types of fracturing are distinguished. Some NNE-SSW to NW-SE border faults and transform NE-SW directional faults of northern Nipouni that cross Pako basin are also highlighted. The border faults of NW-SE direction recognized in Djadja locality (Figure 8 and 9) could be synchronous with the compressive tectonics of N-S direction having affected the Benino-Nigerian block creating the conditions favour able to genesis of basins. Transforming faults could be late fractures that played after genesis of pelvis.

4.1.6. Vertical Gradient (Z-Derivative)

The vertical gradient or first vertical derivative, accentuates the responses of high frequency anomalies and attenuates low frequency anomalies. It's a kind of filter which allows to get a better image of surface structures. In this perspective, we observe the horizontal distribution of major magnetic units, regardless of their position on the vertical plane in the crustal succession in

Pako region. We note the presence of folded structures located in northwest of Nipouni and represented by anomalies of very high magnetic intensity oriented NE-SW. This folding could be synchronous to Panafrican shortening E-W. Two types of fracturing are identified on this map (Figure 10) transforming overall NE-SW directional fractures and simple three-way fractures (NE-SW, NW-SE to E-W). These different fractures are shown in black lines on the map.

4.1.7. Magnetic Fractures Synthesis

Magnetic method allows better imaging of the Earth's structures. In the present study, it helps to confirm certain fractures orientations defined above as lineaments with remote sensing. We note four families of fractures directions. The N-S family grouping the $N0^{\circ}$ to $N20^{\circ}$ fractures make up 14% of the population. NE-SW fractures form 25%. The E-W family contains 32% and the NW-SW fractures form 29% of frequencies. Directional discrimination of magnetic fractures of Pako region shows that N-S faults are oriented $N0^{\circ}$ to $N18^{\circ}$. NE-SW faults are oriented $N28^{\circ}$ to $N51^{\circ}$. E-W family of fractures includes $N72^{\circ}$ to $N90^{\circ}$ directions and NW-SE family of fractures united in $N120^{\circ}$ to $N160^{\circ}$ orientations (Figure 11). Statistical data of these faults shows that E-W orientations are more frequent in Pako region (Figure 11).

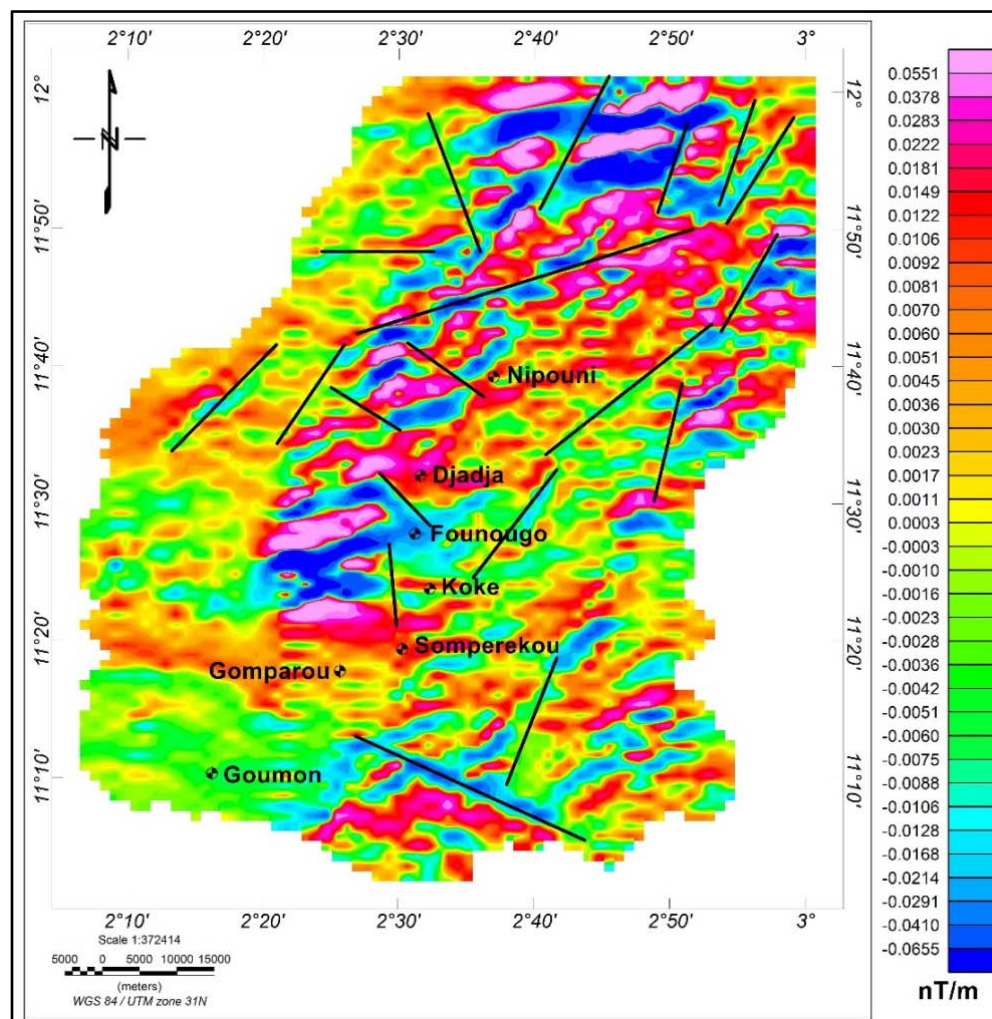


Figure 9. Map of horizontal (y) derivative of total magnetic field reduced to equator in Pako region

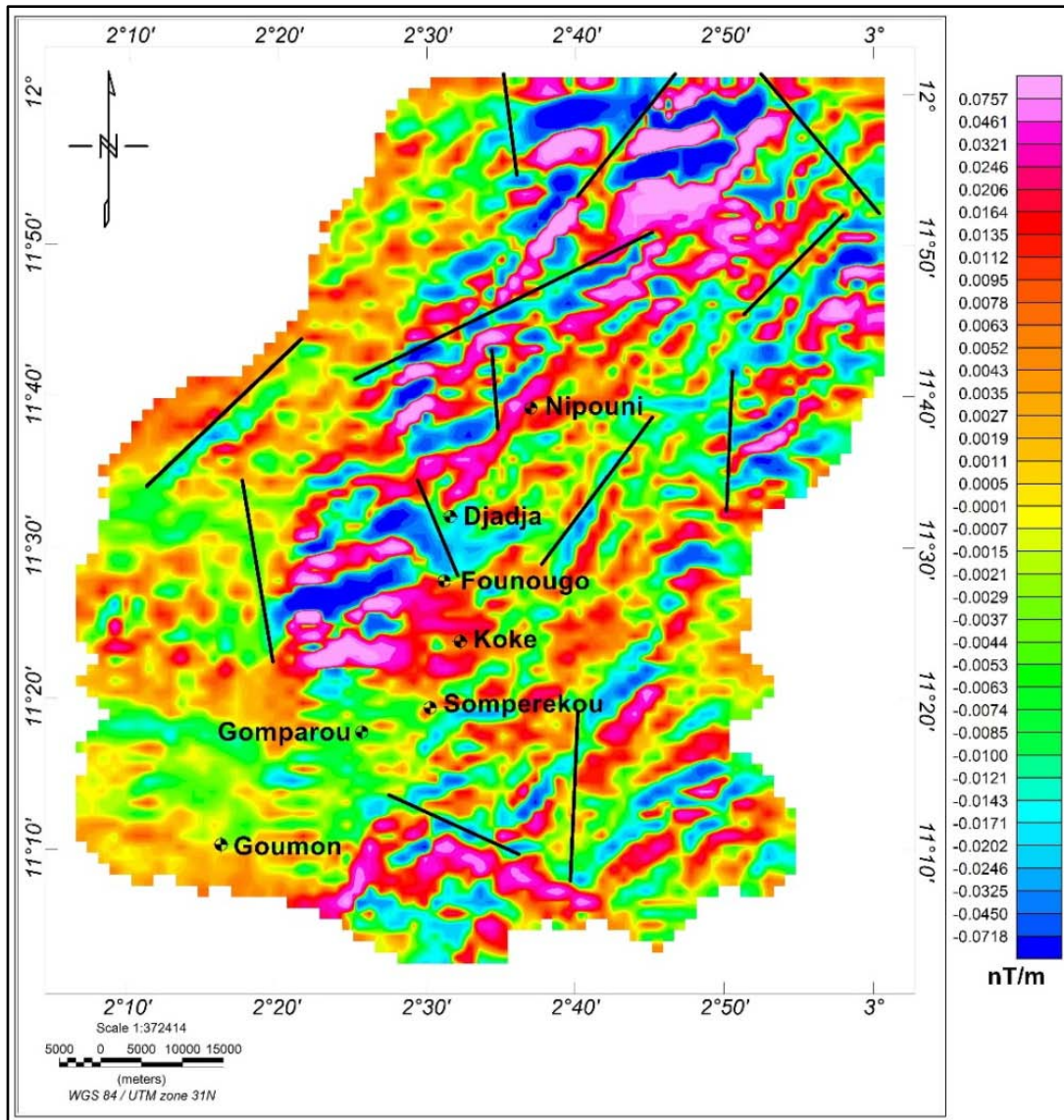


Figure 10. Map of the Vertical (z) gradient of the RTE Magnetic Field of Pako region

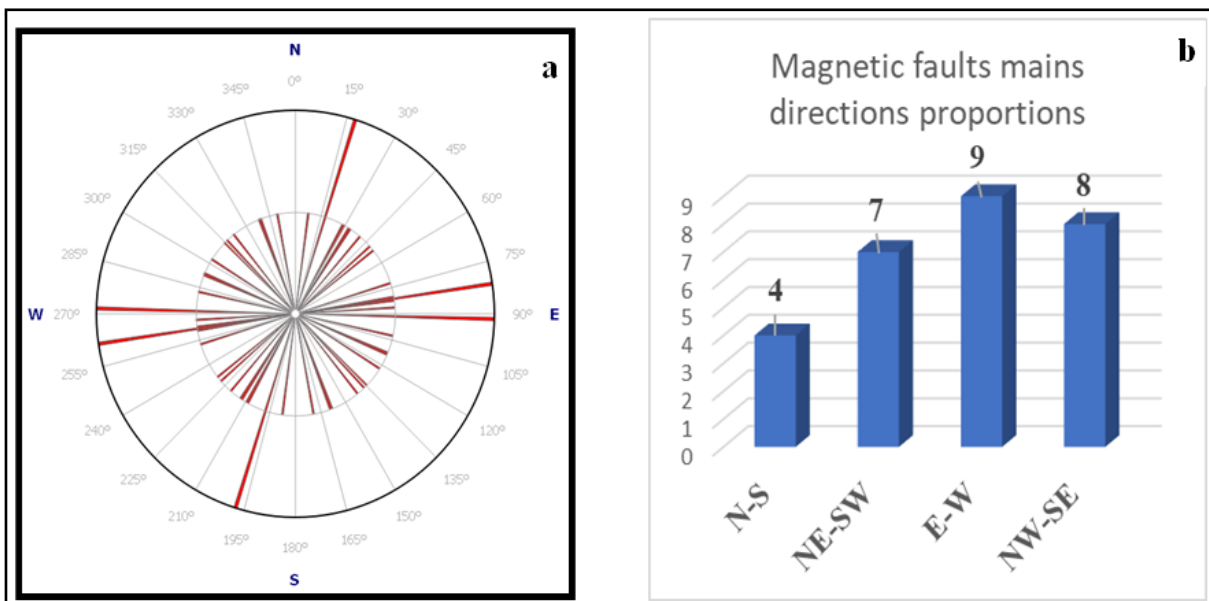


Figure 11. Magnetic faults direction in Pako region a) Rosace diagram b) histogram

A transforming fault NE-SW direction crosses the basin at north of Nipouni. This probably late post-tectonic fracture illustrates a visible dextral displacement on the horizontal (x, y) and vertical (z) gradients maps. Indeed, in gneiss, basalts, metagranites, and gabbros of Wahakourou at north of Nipouni, the presence of microscopic finite deformation markers illustrating a dextral movement was outlined by [21]. Consequently, the existence of NE-SW shear corridors in Pako basin is not exclude. Low intensity shear could involve the secondary directions illustrated on magnetic fault rosace diagram (Figure 11)

4.1.8. Validation of Results

Combine analysis of structures identified by spatial data processing and those obtained with aeromagnetic data confirm the existence of many fractures of various directions in Pako region. Fractures of E-W direction represent 32%. A field campaign, carried out in this region allows us to validate these results. In fact, in Pako region, the N-S oriented amphibolites and sandstone outcrops in south-eastern edge (localities of Somperekou and Brokotto) are associated with concordant fractures (Photo 1a and b). The amphibolites and sandstones of this part of Pako are probably prior to N-S transcontinental shear zone called Kandi in Benin. This deformation, far from being at the origin of Pako basin, affects its formations at its south-eastern border. Referring to map of total magnetic field reduced to equator, these formations have medium to low intensity aeromagnetic signature.

Directions NE-SW to E-W are carried by the Poutigui gneiss (Koke) and the granodiorite dykes associated with concordant veins of basalts located at southwest of Founougo (Photo 2 a and b). Gneisses are characterized by a penetrative schistosity (S1) of foliation. They constitute the oldest basement formations in the region and are affected by Panafrican tangential tectonics responsible for D1 deformation. It is important to note that the gneisses are intruded by moderately to strongly altered mafic rocks

of gabbroic nature. The basalt veins are melanocrate to holomelanocrate (Photo 2b). This part of Pako region is characterized by high to very high aeromagnetic intensity.

Apart fractures and linear structures recognized; other types of deformations are also identified. Unhooking deformations with a dextral rotational component (Photo 3a) and ductile deformations characteristic of folding with development of a schistosity (S2) axial plane (Photo 3b) are also recognized. These structures are generated by D2 deformations. Deformations D2 are noticed in Djadja's schists which are composed of micas with places of concordant veins of pegmatites and characterized by very low aeromagnetic intensity.

4.1.9. Structural Model of Pako Region

Spatial and magnetic data interpretation supported by field observations allowed to propose a structural model of Pako region (Figure 12). Faults are linked to different deformations and can be regrouped into two mains types. Brittles deformations with dextral detachment are observed in the localities of Somperekou and Gomparou while brittle deformations with senestralde tachment and a ductile deformation with a rotational dextral component are observed in Nipouni (Figure 12). The major fractures of global direction NE-SW to NW-SE and those of E-W direction are certainly responsible of collapse led to Pako basin genesis, which they limit on both sides. After setting up of Pako basin, appear characteristic directions of Panafrican events playing in conjugate setbacks, consisting of shears dextral NE-SW to NW-SE and senestral NW-SE (Figure 12). These late setbacks affecting Pako basin can be interpreted as the structures resulting from a reactivation of Kandi shear or discordant structures contemporary to this shear which had not been mapped in previous works. There is a remarkable importance of secondary fractures of various directions throughout the region which can be interpreted as faults without displacement or joints.

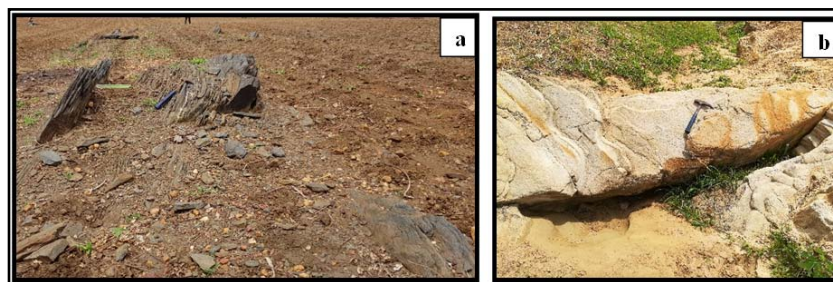


Photo 1. Pako regionsouth-eastern edge rocks fractures: **a)** Amphibolite; **b)** sandstone

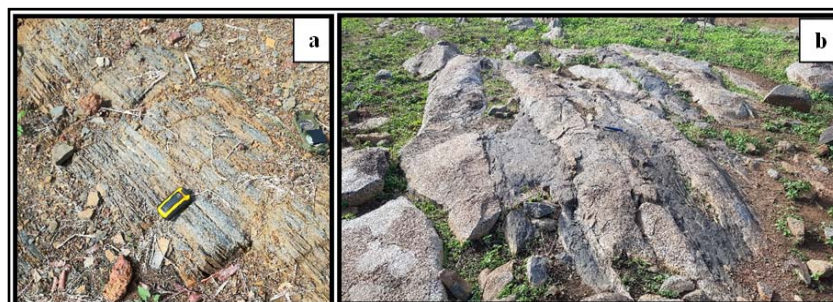


Photo 2. Pako region central edge rocks features: **a)** S1 schistosity in gneiss **b)** granodiorite associated with basalt veins

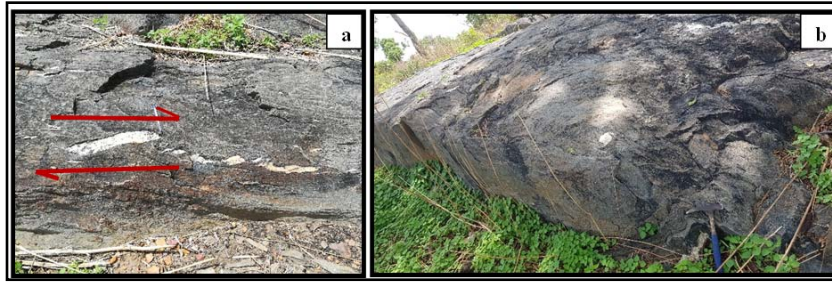


Photo 3. Pako region rocks features: a) schists with dextral shear b) folding

4.2. Discussion

Several authors are agreed with the existence of a large shear corridor in the Benin-Nigerian shield [9,33,34,35,36]. The combined interpretation of Landsat 8 OLI images, magnetic and field data, indicate the existence of at least two phases of deformations in Pako region: N-S to NE-SW brittle or shear deformations and E-W brittle deformations. Identified faults systems are in accordance with those outlined by [37] in Nigeria where the author had considered that they are linked to Panafrican deformations that occurred around 530 Ma across the continent [37]. The brittle deformations observed in Somperekou (Brokotto) locality (Figure 9, 12 and Photo 1) are marked by a system of conjugate N-S fractures forming sometimes, a network of NE-SW to NW-SE fractures (Figure 4). In reality, this

network belongs to a large weakness area of the same orientation.

Within Precambrian rocks of Benin-Nigerian shield, some Panafrican transcurrent faults of varying orientations have been described [23,38,42]. N-S trans current faults are recognized in Kandi, Zungeru and Ifewara areas; NE-SW in Kalanga area and ENE-WSW in Ngaoundere and Benue areas [22,39]. According to [23], the Kandi Shear Zone is of 50km wide and extends in Benin Republic from Malanville to the coastal sedimentary basin. In Dassa region (Benin center), it affects granulite, amphibolite and migmatitic gneisses. Ours field observations show that in the South-east of Pako region, some formations are structured N-S. If these formations are affected by KSZ, it is important to reevaluate the influence zone of this shear corridor because studied formations are more than 50km far from KSZ central zone.

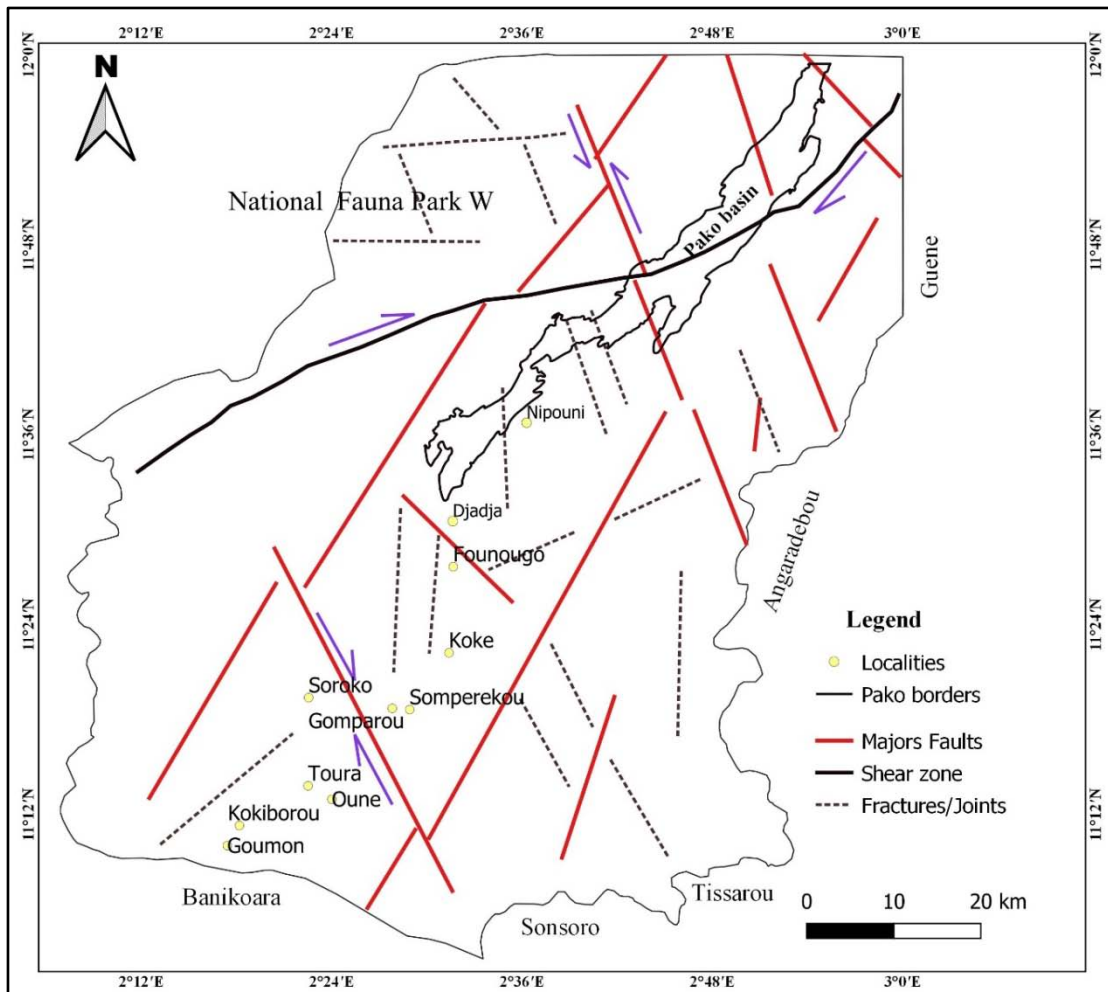


Figure 12. Structural model of Pako region

NE-SW shear directions are also recognized in the basement of Nikki, Djadja and Nipouni regions by some authors [21,42]. Results of the present study gave a synoptic view of deformations at the scale of Pako region. The connection of identified outcrops isolated shears allows to highlight a dextral NE-SW shear corridor in Pako region. These results are in agreement with those of [39] who maps NE-SW shear corridors in the eastern block of Panafrican chain in Nigeria. Thus, NE-SW faults system is linked to regional tectonic event which affect at least the Benino-Nigerian shield.

5. Conclusion

The multi-criteria analysis of Landsat 8 OLI images coupled with magnetic data and their comparison with field data have provided valuable geological informations concerning faults systems of Pako region. Directional Sobel filters results combined with Total magnetic field gradients led to map discontinuities corresponding to the limits of geological formations or to the faults systems in the study area. Their directional discrimination highlights two main directions. The N-S direction structures containing $N0^{\circ}$ to $N18^{\circ}$ fractures and the E-W structures grouping fractures of $N82^{\circ}$ to $N92^{\circ}$ directions. These fractures are the most important in Pako region with a frequency of 32%. Among others fractures, some are oriented NE-SW ($N40^{\circ}$) and define a shear corridor with a dextral rotational component. Based on outlined faults systems, a structural model of this region has been proposed. The use of total magnetic field techniques allowed to highlight magnetic anomalies zones. Magnetic anomalies zones which could represent areas with high mining potential are associated in our study area with Kokometamorphic rocks, Founougo volcanic rocks and Nipounimet asediments. The methodological approach of this study led to map several fractures that were not identified before. Complementary field work should be carried out to measure the magnetic susceptibility of the various rocks in order to confirm magnetic data of Pako region. For geodynamic reconstitution and chronology clarification, geochemical and geochronological studies are necessary.

Acknowledgements

We thank SCHOLA association for financial support and Mr. Evariste AGLI (General Manager of Beninese Office of Geological and Mining Research) for aeromagnetic data provision in carrying out this research work.

References

- [1] Leu, L. K. Use of reduction-to equator process for magnetic data interpretation, in fifty first annual International Meeting, Society of exploration Geophysicists 445 (Abstract) 1981.
- [2] Evans D. Current status and future developments in radar remote sensing. -*ISPRS Journal of Photogrammetry and Remote Sensing*, vol. 47, 79-99. 1992.
- [3] Singhroy V.H.- Radar geology: Techniques and results - *Episodes*, vol. 5.1992.
- [4] Blom R.G., Crippen R.E., Elachi C. - Detection of subsurface features in SEASA Tradarimages of Means Valley, Mojave Desert, California. - *Geology*, vol. 12, 346-349. 1984.
- [5] Sabins F. F. Geologic interpretation of Space Shuttle Radar Images of Indonesia. -*AAPG Bulletin*, 67. 1983.
- [6] Gaddis L., Mougini-Mark R., Singer, Kaupp V. - Geologic analyses of Shuttle Imaging Radar (SIR-B) data of Kilauea Volcano, Hawaii. - *Geological Society of America Bulletin*, vol. 101, 17-332. 1989.
- [7] King C., Feybesse J.-L., Bilia M., Rémond A., Bourguignon A., Rouzeau O., Perrin J., Legendre J. - « AURROS » Radar à Ouverture Synthétique pour l'exploration aurifère. in: Le Programme Aval SAR, ed. CNES DP/OT. 1999.
- [8] Ferre, E. C., Bouchez, J. L., Kozminski, G., & Omitogun, A. A. "SLAR interpretation For structural mapping in the basement of northern Nigeria", Proceedings of the Thematic Conference on Geologic Remote Sensing, vol. 11, no. Ann Arbor, MI, p. I.1996.
- [9] Ferre, E., Gleizes, G., & Caby, R. "Obliquely convergent tectonics and granite emplacement in the Trans-Saharan Belt of eastern Nigeria; a synthesis", *Precambrian Research*, vol. 114, no. 3-4, pp.199-219. 2002.
- [10] Garba, I. "Origin of Pan-African mesothermal gold mineralisation at Bin Yauri, Nigeria", *Journal of African Earth Sciences*, vol. 31, no. 2, pp. 433-449, 2000.
- [11] Garba, I. "Geochemical characteristics of the gold mineralization near Tsohon Birmin Gwari, northwestern Nigeria", *Chemie der Erde*, vol. 62, no. 2, pp. 160-170. 2002.
- [12] Baraou I. S. Contribution à l'étude pétrographique, géochronologique et structurale des formations panafricaines du Sud Maradi (Sud Niger) : relations avec les indices aurifères, these, doctorat, 114p, 2018.
- [13] Prakla Prospection géophysique du Dahomey, reconnaissance au sol des anomalies, 1966.
- [14] Breda. Etude de cartographie géologique et de prospection minière de reconnaissance au Nord du 11e parallèle (Bénin). Rapport final. Projet N°4105-011-13-20, Géomineraria Italiana. 1982.
- [15] Institut Géographique National. Carte topographique du Bénin. 2006.
- [16] Dada, S. S. "Crust-forming ages and Proterozoic crustal evolution in Nigeria; Reappraisal of current interpretations", *Precambrian Research*, vol. 87, no. 1-2, pp. 65-74. 1998.
- [17] Bruguier, O., Dada, S., & Lancelot, J. R. "Early Archaean component (>3.5 Ga) within a 3.05 Ga or thogneiss from northern Nigeria; U-Pb zircon evidence", *Earth and Planetary Science Letters*, vol. 125, no. 1-4, pp. 89-103. 1994.
- [18] Dickin, A. P., Halliday, A. N., & Bowden, P. "A Pb, Sr and Nd isotope study of the basement and Mesozoic ring complexes of the Jos Plateau, Nigeria", *Chemical Geology; Isotope Geoscience Section*, vol. 94, no. 1, pp. 23-32. 1991.
- [19] Kröner, A., Collins, A. S., Hegner, E., Willner, A. P., Muhongo, S., & Kehelpannala, K. V. W. "The East African Orogen: new zircon and Nd ages and implications for Rodinia and Gondwana supercontinent formation and dispersal", *Gondwana Research*, vol. 4, pp. 179-181. 2001.
- [20] Woakes, M., Rahaman, M. A., & Ajibade, A. C. "Some metallogenic features of the Nigerian basement", *Journal of African Earth Sciences* (1983), vol. 6, no. 5, pp. 655-664. 1987.
- [21] Gnammi Y.R. D. I., d'Almeida G.A. F., Kaki C. Lithofaciès et traits structuraux des formations du secteur sud du bassin volcanosédimentaire de la Pako, Nord Bénin, ISS1813-548X, <http://www.afriquescience.net>; 14p. 2020.
- [22] Affaton P., Rahaman M. A., Trompette R., and Sougy J. The Dahomeyide Orogen: Tectono-thermal Evolution and Relationships with the Volta Basin; (1991).
- [23] Adissin Glodji C. L. La zone de cisaillement de Kandi et le magmatisme associé dans la région de Savalou-Dassa (Bénin): étude structurale, pétrologique et géochronologique. Thèse de Doctorat, Université de Lyon, 224 pages. 2012.
- [24] Drury S. A. Remote sensing of geological structure in temperate agricultural terrain. *Geological Magazine*. 123(2) 113-121. 1986.
- [25] Marion A. Introduction aux techniques de traitement d'image. Paris, Editions Eyrolles, 278p. 1987.
- [26] Toutin T. La correction géométrique rigoureuse : un mal nécessaire pour la santé des résultats. *Journal canadien de télédétection*, Vol. 22(2) 184-189. 1996.

- [27] Bonn, F. et Rochon, G. Précis de Télédétection. Principes et méthodes. Presse de l'université de Québec / AUPELF, vol. 1, 485 p. 1992.
- [28] Ranjbar H, Honarm M and Moezifar Z. Analysis of ETM+ and Airborne Geophysical Data for Exploration of Porphyry Type Deposits in the Central Iranian Volcanic Belt, Using Fuzzy Classification, Remote Sensing for Environmental Monitoring, GIS Applications, and Geology III, SPIE pp. 165-173. 2004).
- [29] Chabrilat S, Pinet P, Ceuleneer G, Johnson P and Mustard J. Ronda Peridotite Massif: Methodology for its Geological Mapping and Lithological Discrimination from Airborne Hyperspectral Data, International Journal of Remote Sensing 21(12), 2363-2388. 2000.
- [30] Pinet P., Shevchenko V., Chevrel S., Daydou Y. and Rosemberg C. Local and Regional Lunar Regolith Characteristics at Reiner Gamma Formation: Optical and Spectroscopic Properties from Clementine and Earth-Based Data, Journal of Geophysical Research 105, 9457-9475. 2000.
- [31] Blakely, R.J., Simpson, R.W., Locating edges of source bodies from magnetic or gravity anomalies. Geophysics 51 (14), 94-98. 1986.
- [32] Kouamé K. F., Lasm T., Saley M. B., Tonyé E., Bernier M. & Wade, S. Extraction linéaire par morphologie mathématique sur une image RSO de RadarSat-1: Application au socle Archéen de la Côte d'Ivoire, III^{ème} Journées d'Animation Scientifique du réseau de Télédétection de l'AUF JAS'09, Sous le thème: « Imagerie Satellitaire Multisources : Approches Méthodologiques et Applications », Alger, 8-11 novembre 2009.
- [33] Caby R. and J.M. Boessé J. M. Pan-African nappe system in southwest Nigeria: the Ife-Ilesha schist belt. Journal of African Earth Sciences, Vol 33, N° 2, pp. 211-225. 2001.
- [34] Affaton P., Gaviglio P. and Pharisaat A. Réactivation du craton ouest-africain au Panafricain : paléocontraintes déduites de la fracturation des grès néoproterozoïques de Karey Gorou (Niger, Afrique de l'Ouest). C. R. Acad. Sci. Paris, Sciences de la Terre et des planètes / Earth and Planetary Sciences 331 (2000) 609-614. 2000.
- [35] Tairou M. S., Affaton P., Gélard P., Aïté R. and Sabi E. Panafrican brittle deformation and palaeo-stress superposition in northern Togo (West Africa). C. R. Geoscience 339. (2007) 849-857. 2007.
- [36] Chala D., Tairou M.S., Wenmenga U., Kwékam M., Affaton P., Kalsbeek F. and Tossa C., Houéto A. Pan-African deformation markers in the migmatitic complexes of Parakou-Nikki (Northeast Benin). *Journal of African Earth Science*, 111 (2015), 387-398. 2015.
- [37] Ball. E. An example of very consistent brittle deformation over a wide intracontinental area: the late Pan-African fracture system of the Tuareg and Nigerian shield. *Tectonophysics*, 16, (1980) 363-379 p. 1980.
- [38] Mc Curry P. Pan-african orogeny in Northern Nigeria. - *Geol. Soc. Amer. Bull.*, 80, 1775-1782. 1971.
- [39] Chukwu-Ike M. I. Régional photogéologique interpretation of tectonic features of central Nigeria basement complex: A satellite imagery based study, Mc., Dic PhD, 1997.
- [40] Affaton P. Notice explicative des cartes géologiques au 1 / 200 000 de la République populaire du Bénin entre les 9° et 10° degrés de latitude nord (feuille de Bassari-Djouguet feuille de Parakou-Nikki). Rapport B.R.G.M., n° 78 RDM055AF, Orléans, Fr, 70 p., cartes, 2 annexes, inédit, 1978.
- [41] Caby R., Black R., Mousine-Pouchkine A., Bayer R., Bertrand M.J., Boullier M. A., Fabre J. and Lesquer A. Evidence for late Precambrian plate tectonics in West Africa, 5p. 1981.
- [42] Affaton P., Tairou M. S., Tossa C., Chala D. and Kwékam M. Premières données microstructurales sur le complexe granito-migmatitique de la région de Nikki, Nord Est Bénin, 14p. LTD printed in Nigeria ISSN 1596-6798 www.globaljournalseries.com, 2013.

